

The Carbon–Lithium Bond in Monomeric Aryllithiums: Dynamics of Exchange, Relaxation, and Rotation

Gideon Fraenkel,* Sheela Subramanian, and Albert Chow

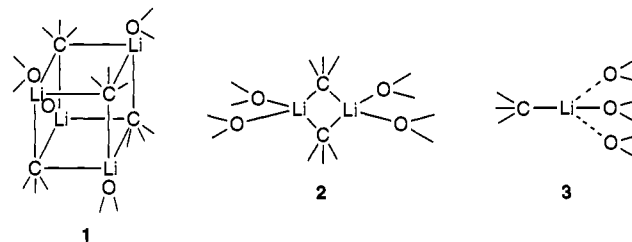
Contribution from the Department of Chemistry, Ohio State University, Columbus, Ohio 43210

Received January 18, 1995[Ⓢ]

Abstract: Carbon-13 NMR line shape analysis of the lithium isotopomers of 2,4,6-tri-*tert*-butylphenyllithium monomer, **4**, complexed to THF establishes that electric quadrupole induced relaxation of ⁷Li is responsible for partial averaging of ¹J(¹³C,⁷Li). The dynamics of intramolecular carbon–lithium bond exchange between monomers of **4** in THF solutions have been monitored by NMR line shape analysis, signal averaging of ¹J(¹³C,⁶Li) observed above 240 K, yielding activation parameters of Δ*H*[‡] and Δ*S*[‡] of respectively 14.4 kcal/mol and 7 eu. All except the *meta* carbons of mesityllithium, **5**, monomer tridentately complexed to *N,N',N'',N'''*-pentamethyldiethylenetriamine, PMDTA, are magnetically non-equivalent at 184 K, supporting an asymmetric structure in which lithium is chiral. With increasing temperature above 184 K the shifts between the *ortho* ring carbons, the *ortho* methyls, and two doublets due to methylenes progressively average to single lines at their respective centers, the result of increasingly fast rotation around the carbon–lithium bond, with resulting activation parameters of Δ*H*[‡] and Δ*S*[‡] of respectively 5 kcal/mol and –21 eu. It is proposed that rotation is chemically driven, the result of Li, N reversible dissociation accompanied by an uptake by Li of one THF molecule.

NMR studies of organolithium structure are based on the existence of scalar coupling between ¹³C and directly bonded ⁶Li.^{1,2} For a RLi compound prepared enriched 96% in ⁶Li the multiplicity of the ¹³C resonance for carbon bonded to lithium indicates how many lithiums are bonded to that particular carbon, i.e. information on structure.^{3,4} With increasing temperature intermolecular carbon–lithium bond exchange becomes fast enough to average ¹J(¹³C,⁶Li), so NMR line shape analysis can be used to study dynamics of this process.^{3b,5,6} An example of this procedure is shown below. Lithium-7 cannot be used in these experiments since quadrupole relaxation is fast enough^{3a,7} to average out ¹J(¹³C,⁷Li). Under favorable circumstances line shape analysis of ⁷Li-bound ¹³C provides dynamic information on the ⁷Li relaxation process; an example is given below. As a result of NMR^{2–4} and X-ray crystallographic⁸ studies many solvated organolithium compounds have been shown to consist of just cubic tetramers, bridged dimers, or most recently

monomers or some equilibrium mixture of two to three of these, see **1** to **3**. Interconversions in the direction of smaller more



solvated species are exothermic and entropically negative.^{2b,3b} While diethyl ether and tertiary monoamines favor formation of tetramers, dimers, bidentately complexed to vicinal diamines such as *N,N,N',N''*-tetramethylethylenediamine, TMEDA, predominate at lower temperatures,^{3a,4} finally triamines, for example, pentamethyldiethylenetriamine, PMDTA, tend to form tridentately complexed monomeric organolithium compounds.⁹ These remarks also generalize the structural variety of aryllithiums. For example, X-ray crystallography showed complexes of phenyllithium separately with diethyl ether, TMEDA, and PMDTA to be respectively tetramer,¹⁰ dimer,¹¹ and monomer.¹² Carbon-13 NMR of diethyl ether solutions, at low temperature, established the TMEDA complex to be a bidentately complexed bridged dimer^{3a} while that in THF is an equilibrium mixture of dimer and monomer.⁹ Recently with use of ¹³C NMR, 2,4,6-tri-*tert*-butylphenyllithium (**4**) in THF and mesityllithium (**5**) with PMDTA in THF were both shown

[Ⓢ] Abstract published in *Advance ACS Abstracts*, May 15, 1995.

(1) (a) Fraenkel, G.; Fraenkel, A. M.; Geckle, M. J.; Schloss, F. *J. Am. Chem. Soc.* **1979**, *101*, 4745–4747. (b) Fraenkel, G.; Henrichs, M.; Hewitt, J. M.; Su, B. M.; Geckle, J. M. *J. Am. Chem. Soc.* **1980**, *102*, 3345–3350.

(2) (a) Seebach, D.; Hassig, R.; Gabriel, J. *Helv. Chim. Acta* **1983**, *66*, 308. (b) Seebach, D.; Siegel, H.; Gabriel, J.; Hässig, R. *Helv. Chim. Acta* **1980**, *63*, 2046–2053.

(3) (a) Fraenkel, G.; Hsu, H.-P.; Su, B. M. In *Lithium Current Applications in Science Medicine and Technology*; Bach, R. O., Ed.; Wiley: New York, 1985; p 273. (b) Fraenkel, G. In *Recent Advances in Anionic Polymerization*; Hogen-Esch, T., Smid, J., Eds.; Elsevier: New York, 1987; p 23.

(4) (a) Reviewed by Bauer, W.; Schleyer, P. v. R. In *Advances in Carbanion Chemistry*; Sniekus, V., Ed.; Jai Press: Greenwich, CT, 1992; Vol. 1, pp 81–175. (b) Gunther, H.; Moskau, D.; Bast, P.; Schmaltz, D. *Angew. Chem., Int. Ed. Engl.* **1987**, *26*, 1212. (c) Thomas, R. D. In *Isotopes in the Physical and Biomedical Sciences*; Jones, J. R., Buncl, E., Eds.; Elsevier, Amsterdam, 1992; p 367.

(5) Exchange effects: Thomas, R. D.; Clark, M. T.; Jensen, R. M.; Young, T. C. *Organometallics* **1986**, *5*, 1851.

(6) Fraenkel, G. In *Techniques in Chemistry, Investigations of Rates and Mechanisms, of Reactions*, 4th ed.; Bernasconi, C. F., Ed.; Wiley-Interscience: New York, 1986; Part 2, pp 357–604.

(7) Pople, J. A.; Schneider, W. G.; Bernstein, H. J. In *High Resolution Nuclear Magnetic Resonance*; McGraw-Hill Book Company Inc.: New York, 1959; p 480.

(8) Reviewed: (a) Williard, P. G. In *Comprehensive Organic Synthesis, Selectivity Strategy and Efficiency in Organic Chemistry*; Trost, B. M., Fleming, I., Eds.; Pergamon-Press: Oxford, 1991; pp 1–48. (b) Setzer, W. M.; Schleyer, P. v. R. *Adv. Organomet. Chem.* **1985**, *24*, 353.

(9) Bauer, W.; Winchester, W. R.; Schleyer, P. v. R. *Organometallics* **1987**, *6*, 2371–2379.

(10) Hope, H.; Power, P. P. *J. Am. Chem. Soc.* **1983**, *105*, 5320.

(11) Thonnes, D.; Weiss, E. *Chem. Ber.* **1978**, *111*, 3157.

(12) Schuman, U.; Kopf, J.; Weiss, E. *Angew. Chem., Int. Ed. Engl.* **1985**, *24*, 215.

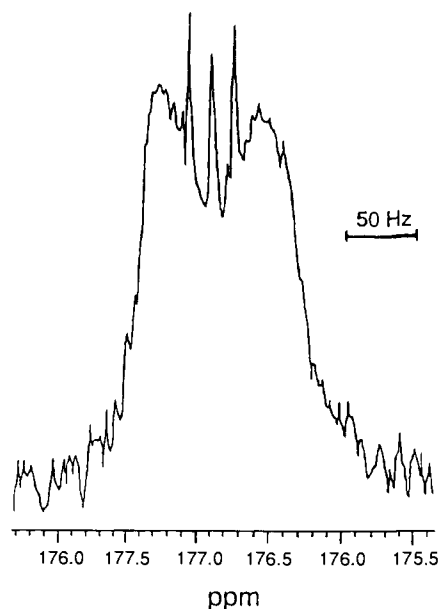
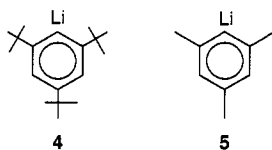


Figure 1. ^{13}C NMR of C_1 of 2,4,6-tri-*tert*-butylphenyllithium at 200 K; (reprinted with permission from ref 9).

to be monomers.⁹ The two aromatic compounds exhibited



interesting NMR line shape behavior indicative of dynamic processes such as intermolecular carbon–lithium bond exchange, ^7Li relaxation, and rotation about the C, Li bonds. That is the subject of this article.

Results and Discussion

Bauer, Winchester, and Schleyer reported⁹ that the *ipso* ^{13}C resonance of 2,4,6-tri-*tert*-butylphenyllithium (**4**) (^7Li and ^6Li in natural abundance, in THF-D_8) at 200 K consists of a well-resolved narrowly-spaced 1:1:1 triplet due to $^1J(^{13}\text{C}, ^6\text{Li}) = 16.4$ Hz from the *ca.* 7% ^6Li isotopomer, superposed on what looks like a broad featureless doublet with a separation of 70 Hz due to ^7Li -bound ^{13}C (see Figure 1). The appearance of the triplet indicates that the prevailing species is a monomer in THF and that at 200 K both intermolecular carbon–lithium bond exchange and ^6Li scalar relaxation of the second kind are slow relative to the NMR time scale.^{2,3} In contrast, the broad doublet is not just the result of line broadening of the outer components of a quartet due to $^1J(^{13}\text{C}, ^7\text{Li})$. The spin of ^7Li is $3/2$. Under circumstances of slow intermolecular C, Li bond exchange and slow ^7Li relaxation the $^{13}\text{C}_{\text{ipso}}$ resonance of the ^7Li isotopomer of **4** should consist of an equally placed 1:1:1:1 quartet with $^1J(^{13}\text{C}, ^7\text{Li})$, of 43.31 Hz based on the observed value of $^1J(^{13}\text{C}, ^6\text{Li}) = 15$ Hz. Thus the broad doublet due to C_{ipso} of **4** ^7Li is not just the result of line broadening of the outer components of the just-mentioned equal quartet. That separation should be 128.4 Hz; however, the authors report 70 Hz.⁹ Therefore this broad doublet must arise from some relaxation process. Under favorable circumstances the nature of the process can be determined by means of NMR line shape calculations.^{13,14}

(13) (a) Bloch, F. *Phys. Rev.* **1956**, *102*, 104. (b) Bloch, F. *Phys. Rev.* **1957**, *105*, 1206. (c) Kaplan, J. I. *J. Chem. Phys.* **1971**, *55*, 1489. (d) Redfield, A. G. *Adv. Magn. Reson.* **1965**, *1*, 1–32.

Table 1. $\langle l|q|m\rangle = \rho_n$

$^{13}\text{C}^6\text{Li}$			$^{13}\text{C}^7\text{Li}$		
l	m	n	l	m	n
$\alpha (+1)$	$\beta (+1)$	1	$\alpha (+3/2)$	$\beta (+3/2)$	4
$\alpha (0)$	$\beta (0)$	2	$\alpha (+1/2)$	$\beta (+1/2)$	5
$\alpha (-1)$	$\beta (-1)$	3	$\alpha (-1/2)$	$\beta (-1/2)$	6
			$\alpha (-3/2)$	$\beta (-3/2)$	7

Elements of the density matrix required to calculate the ^{13}C NMR line shapes^{6,13–15} of pseudospecies $^{13}\text{C}^6\text{Li}$ and $^{13}\text{C}^7\text{Li}$ are diagonal in lithium and off diagonal, $\Delta m = +1$, in ^{13}C . Summation

$$\langle \alpha \phi_{\text{Li}} | \rho | \beta \phi_{\text{Li}} \rangle \quad (1)$$

of the imaginary parts of these elements gives the absorption (2).

$$\text{Abs}(\omega) = -\text{Im} \sum_{\phi_{\text{Li}}} \langle \alpha \phi_{\text{Li}} | \rho | \beta \phi_{\text{Li}} \rangle \quad (2)$$

The elements $\rho_{l,m}$ are obtained by solving the coupled equations,^{6,16} generated from the corresponding elements

$$\langle \alpha \phi_{\text{Li}} | \dot{\rho} | \beta \phi_{\text{Li}} \rangle \quad (3)$$

of the density matrix equation, (4),

$$\dot{\rho} = i[\rho, \mathcal{H}] - \frac{\rho}{T} + \mathbf{R}\rho = 0 \quad (4)$$

in which \mathcal{H} is the hamiltonian in the rotating frame, in radians/s, given as (5),

$$\mathcal{H} = 2\pi(\nu_{\text{C}} - \nu)I_{\text{C}}^z + 2\pi J_{\text{CLi}}I_{\text{C}}^z I_{\text{Li}}^z + 2\pi\nu_1 I_{\text{C}}^x \quad (5)$$

$1/T$ is the phenomenological line width parameter, ν_1 is the RF power, and \mathbf{R} is the appropriate relaxation operator^{13,14} given as

$$\mathbf{R}\rho = \sum_j j_{\alpha} [\mathcal{I}_{\alpha}, [\mathcal{I}_{-\alpha}, \rho]] \quad (6)$$

wherein j_{α} 's are spectral densities and \mathcal{I}_{α} 's are spin operators associated with different relaxation mechanisms. In these calculations we use the spin product representation and elements of the relaxation operators are evaluated at the extreme narrowing approximation.¹⁷

Table 1 lists the required elements of the density matrix for both systems. States of lithium have been abbreviated by their m_z values.

Elements of the density matrix equations take the form

$$i[\mathcal{H}_{m,m} - \mathcal{H}_{l,l}]\rho_{l,m} - \frac{\rho_{l,m}}{T} + [\mathbf{R}\rho]_{l,m} = -iC \quad (7)$$

where C is a constant. The resulting equations are solved for the ρ elements and absorption obtained using (2). For each of the pseudospecies $^{13}\text{C}^6\text{Li}$ or $^{13}\text{C}^7\text{Li}$ undergoing relaxation via a particular mechanism only the relaxation operator need be

(14) (a) Abragam, A. In *The Principles of Nuclear Resonance*; Oxford University Press: London, 1961; Chapter 8; (b) Kaplan, J. I.; Fraenkel, G. In *NMR of Chemically Exchanging Systems*; Academic Press: New York, 1980; Chapter 4.

(15) (a) Kaplan, J. I. *J. Chem. Phys.* **1958**, *28*, 278, 462. (b) Kaplan, J. I.; Fraenkel, G. *J. Am. Chem. Soc.* **1972**, *94*, 2907.

(16) (a) Gutowsky, H. S.; Saika, A. *J. Chem. Phys.* **1953**, *21*, 1688. (b) Gutowsky, H. S.; Holm, C. H. *J. Chem. Phys.* **1957**, *25*, 1288. (c) Johnson, C. S. *Adv. Magn. Reson.* **1965**, *1*, 33.

(17) Reference 14b, p 45.

changed; the frequency and $1/T$ terms in the coefficient matrix are common to all three sets of equations which each take account, separately, of dipole–dipole, chemical shift anisotropy or quadrupole induced relaxation, respectively. Density matrix equations in matrix form for the system $^{13}\text{C}^6\text{Li}$ which includes the effects of dipole–dipole relaxation are displayed in (8).

$$\begin{bmatrix} i2\pi(\Delta\nu - J_6) & 0.6r_d & 0 \\ 1/T - 2.1r_d & & \\ 0.6r_d & i2\pi\Delta\nu - 1/T & 0.6r_d \\ & -4.4r_d & \\ 0 & 0.6r_d & i2\pi(\Delta\nu + J_6) \\ & & -1/T - 2.1r_d \end{bmatrix} \begin{bmatrix} \rho_1 \\ \rho_2 \\ \rho_3 \end{bmatrix} = iC \begin{bmatrix} 1 \\ 1 \\ 1 \end{bmatrix} \quad (8)$$

The corresponding equations which take account of relaxation induced by the ^6Li quadrupole moment and via anisotropy of the chemical shift are obtained by replacing the relaxation coefficient matrix in (8) by \mathbf{R}_q (9) and \mathbf{R}_c (10), respectively.

$$\mathbf{R}_q = \begin{bmatrix} -8j_q & 4j_q & 4j_q \\ 4j_q & -8j_q & 4j_q \\ 4j_q & 4j_q & -8j_q \end{bmatrix} \quad (9)$$

$$\mathbf{R}_c = \begin{bmatrix} 4j_c & 4j_c & 0 \\ 4j_c & -8j_c & 4j_c \\ 0 & 4j_c & -4j_c \end{bmatrix} \quad (10)$$

Since conditions of extreme narrowing are assumed it is possible to express spectral densities for each relaxation mechanism in terms of a single dynamic parameter, r_d , j_q , j_c , see (11) and (13),

$$r_d = \frac{(u_Q \hbar \gamma_C \gamma_{\text{Li}})^2 \tau_d}{(4\pi r_{\text{CLi}})^2} \quad (11)$$

$$j_q = \frac{0.3(e^2 q Q)^2 \tau_q}{(4\pi I(2I - 1)\hbar)^2} \quad (12)$$

$$j_c = 0.041(\Delta\sigma\omega)^2 \tau_c \quad (13)$$

wherein c, d, and q stand for chemical shift anisotropy and dipole–dipole and quadrupole interactions, respectively; γ 's are gyromagnetic ratios; r_{CLi} is the C–Li bond length; $\Delta\sigma$ is the anisotropy of the chemical shift; and τ 's are correlation times.^{13,14}

The density matrix equation in matrix form for $^{13}\text{C}^7\text{Li}$ needed to calculate the ^{13}C NMR, subject to Li quadrupole induced relaxation, is shown in (14).

$$\begin{bmatrix} i2\pi(\Delta\nu - 3/2J) & 24j_q & 24j_q & 0 \\ -1/T - 48j_q & & & \\ 24j_q & i2\pi(\Delta\nu - 1/2J) & 0 & 24j_q \\ & -1/T - 48j_q & & \\ 24j_q & 0 & i2\pi(\Delta\nu + 1/2J) & 24j_q \\ & & -1/T - 48j_q & \\ 0 & 24j_q & 24j_q & i2\pi(\Delta\nu + 3/2J) \\ & & & -1/T - 48j_q \end{bmatrix} \times \begin{bmatrix} \rho_1 \\ \rho_2 \\ \rho_3 \\ \rho_4 \end{bmatrix} = -iC \begin{bmatrix} 1 \\ 1 \\ 1 \\ 1 \end{bmatrix} \quad (14)$$

Relaxation matrices for this system subject to the dipole–dipole

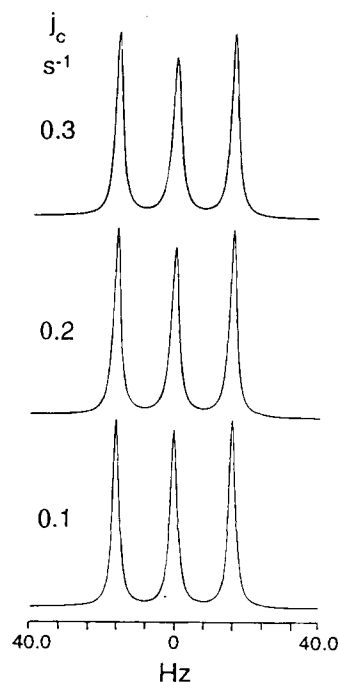


Figure 2. ^{13}C NMR calculated line shapes of $^{13}\text{C}^6\text{Li}$, $J(^{13}\text{C}, ^6\text{Li}) = 16.4$ Hz, subject to ^6Li relaxation by anisotropy of the chemical shift (csa), at different rates, j_c (see text); extreme narrowing limit.

and chemical shift anisotropy mechanisms are shown in (15) and (16).

$$\mathbf{R}_c = \begin{bmatrix} -6j_c & 6j_c & 0 & 0 \\ 6j_c & -14j_c & 8j_c & 0 \\ 0 & 8j_c & -14j_c & 6j_c \\ 0 & 0 & -6j_c & -6j_c \end{bmatrix} \quad (15)$$

$$\mathbf{R}_d = \begin{bmatrix} -6.45r_d & 0.9r_d & 0 & 0 \\ 0.9r_d & -5.05r_d & 1.2r_d & 0 \\ 0 & 1.2r_d & -5.05r_d & 0.9r_d \\ 0 & 0 & 0.9r_d & -6.45r_d \end{bmatrix} \quad (16)$$

That the $^{13}\text{C}_{\text{ipso}}$ resonance of $4\text{-}^6\text{Li}$ is a well-resolved triplet¹⁸ puts an upper limit on the relaxation rate due to dipole–dipole (dd) and chemical shift anisotropy (csa) interactions to which the species might be subject. Inspection of relaxation terms in the elements of the coefficient matrices in (8) and (10) shows qualitatively that quite slow rates of relaxation would broaden the central line of the triplet compared to the outer ones. This is seen more clearly in calculated line shapes for $^{13}\text{C}_{\text{ipso}}$ (C–Li) of $4\text{-}^6\text{Li}$ which take account of dd and csa relaxation, see Figures 2 and 3. Allowing for intrinsic line widths of 2 to 4 Hz, use of values of j_c and r_d as low as 0.2 s^{-1} still results in selective broadening of the central component of the $^{13}\text{C}_{\text{ipso}}$ triplet. Thus the upper limit to j_c and r_d should be no more than 0.1 s^{-1} . Assuming limiting values of 0.1 s^{-1} for j_c and r_d for $^{13}\text{C}_{\text{ipso}}$ in $4\text{-}^6\text{Li}$, one can estimate the corresponding relaxation parameters which apply to the $4\text{-}^7\text{Li}$ isotopomer using the known ratios of composite spectral densities (11) to (13); both are 6.98.^{13,14}

(18) The ^{13}C NMR of $4\text{-}^6\text{Li}$ shows C_{ipso} clearly as 1:1:1 equally spaced triplet.

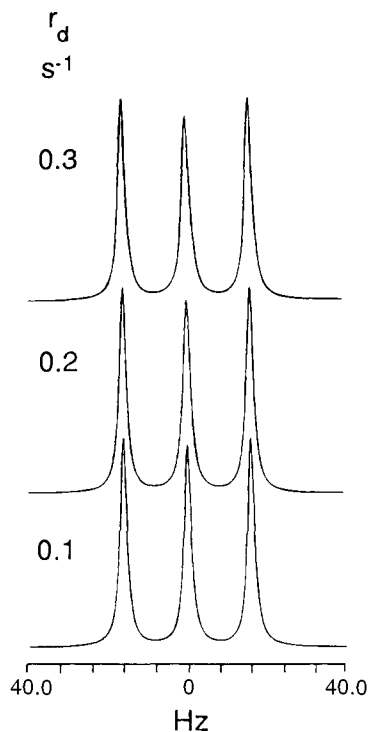


Figure 3. ^{13}C NMR as in Figure 2 as a function of dipole–dipole (dd) relaxation rate, r_d , see text.

$$\frac{j_{c(^{7}\text{Li})}}{j_{c(^{6}\text{Li})}} = \frac{r_{d(^{7}\text{Li})}}{r_{d(^{6}\text{Li})}} = \frac{(\nu_{^7\text{Li}})^2}{(\nu_{^6\text{Li}})^2} \quad (17)$$

Then the maximum dynamic parameters j_c and r_d which apply to $4\text{-}^7\text{Li}$ should be no more than 0.7 s^{-1} . Using this value together with a $^1J(^{13}\text{C}, ^7\text{Li})$ of 43.3 Hz, as obtained above, $^{13}\text{C}_{\text{ipso}}$ NMR line shapes were calculated for $4\text{-}^7\text{Li}$, subject to dipole–dipole (dd) and chemical shift anisotropy (csa) interactions (see Figure 4). From the well-resolved appearance of the $^{13}\text{C}_{\text{ipso}}$ quartets it is clear that dd and csa relaxation are not responsible for the experimental line shapes of $4\text{-}^7\text{Li}$.

Carbon-13 line shapes for $^{13}\text{C}_{\text{ipso}}$ of $4\text{-}^7\text{Li}$ were also calculated, at the extreme narrowing approximation, taking into account ^7Li quadrupole induced relaxation (see Figure 5). As j_q increases the left- and right-hand pairs of lines progressively average to broad lines at their respective centers. The line shape calculated for $j_q = 0.6\text{ s}^{-1}$ most closely resembles the experimental spectrum (see Figures 1 and 5). Thus ^7Li induced quadrupole relaxation is most likely responsible for the partial signal averaging of the $^{13}\text{C}_{\text{ipso}}$ quartet in $4\text{-}^7\text{Li}$. This conclusion also applies to similar results reported by Seebach et al. on ^{13}C NMR of carbon-bound lithium (isotopes in natural abundance) in 7-iodo-7-lithiobicyclo[4.1.0]heptane^{2b} and in ^{31}P NMR of the 2-lithio-1,3-dithiane · HMPT complex at $-135\text{ }^\circ\text{C}$ in 3:2 THF/dimethyl ether.¹⁹

2,4,6-Tri-*tert*-butylphenyllithium- ^6Li ($4\text{-}^6\text{Li}$) was prepared by exchanging the corresponding bromides with *n*-butyllithium- ^6Li in diethyl ether at $0\text{ }^\circ\text{C}$.²⁰ After ether and bromide were removed the lithium compound, $4\text{-}^6\text{Li}$, was dissolved in THF- D_8 with a molar equivalent of *N,N,N',N',N''*-pentamethyldiethylenetriamine, PMDTA, for subsequent NMR study. Figure 6 compares ^{13}C shifts of $4\text{-}^6\text{Li}$ in THF- D_8 with data for THF- D_8 solution containing a molar equivalent of PMDTA. The

(19) Reich, H. J.; Borst, J. P.; Dykstra, R. R. *Tetrahedron* **1994**, *20*, 5873.

(20) A variation of the procedure in ref 9, p 2379.

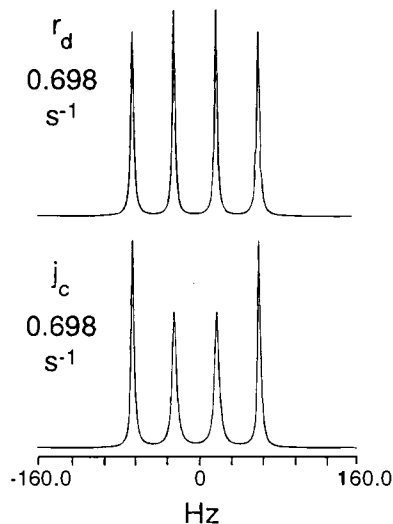


Figure 4. (Bottom) ^{13}C NMR calculated line shapes of $^{13}\text{C}^7\text{Li}$, $J(^{13}\text{C}, ^7\text{Li})$ of 43.3 Hz, subject to ^7Li relaxation via anisotropy of the chemical shift (csa), at different rates, j_c (see text); extreme narrowing limit. (Top) ^{13}C NMR calculated line shapes as in Figure 4 as a function of dipole–dipole (dd) relaxation rate, r_d , see text.

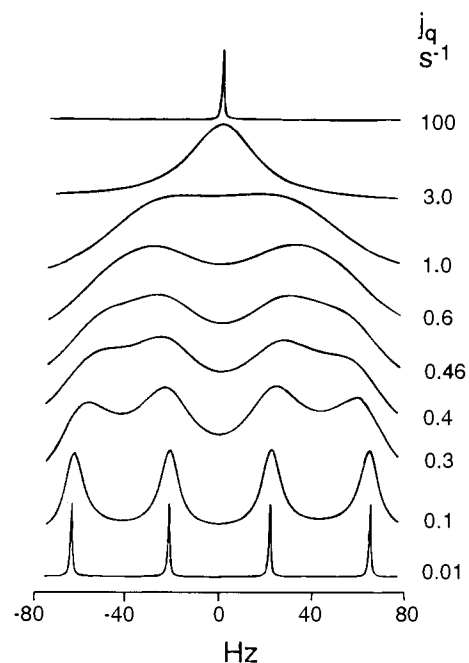


Figure 5. Calculated ^{13}C NMR line shapes for $^{13}\text{C}^7\text{Li}$ as in Figure 4, as a function of the ^7Li quadrupole relaxation rate, j_q , see text.

shifts for contained PMDTA at (δ values) 46.61 (dimethylamino), 43.54 (*N*-methyl), 58.77 and 57.89 (methylene) are quite similar to shifts for free triamine at 46.2 (dimethylamino), 43.03 (*N*-methyl), and 58.32 and 57.46 (methylenes). Hence one can conclude that **4** is not complexed to PMDTA but rather to THF- D_8 , as is the case for phenyllithium in THF. Up to 240 K $^{13}\text{C}_{\text{ipso}}$ NMR of $4\text{-}^6\text{Li}$ in THF- D_8 consists of a 1:1:1 triplet due to $^1J(^{13}\text{C}, ^6\text{Li})$ of 15.7 Hz, indicating the compound is most likely a THF-solvated monomer. Above 240 K with increasing temperature this coupling is progressively averaged so that by 271 K the resonance consists of a single sharp peak (see Figure 7). This effect is either the result of some fast ^6Li relaxation process or it arises from bimolecular carbon lithium bond exchange. The former is unlikely since ^6Li relaxation tends to be very slow.²¹

(21) Wehrli, F. W. *J. Magn. Reson.* **1978**, *30*, 193.

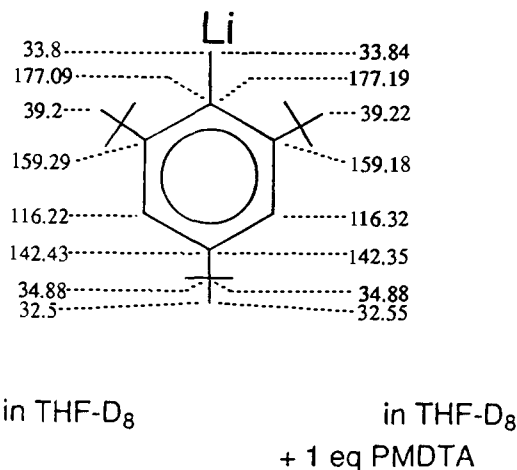


Figure 6. ^{13}C NMR shifts of $4\text{-}^6\text{Li}$: (left) in THF-D_8 ; (right) in THF-D_8 with 1 mol equiv of PMDTA.

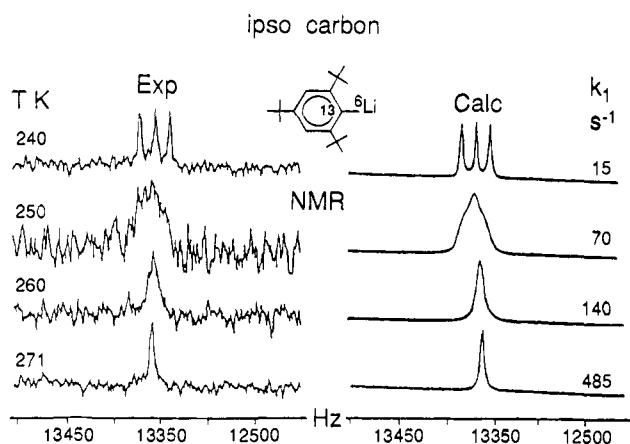


Figure 7. ^{13}C NMR line shapes $^{13}\text{C}_{\text{ipso}}$ of $4\text{-}^6\text{Li}$ in THF-D_8 ; (left) experimental values at different temperatures; (right) calculated to fit, subject to bimolecular exchange.

Density matrix equations were derived to calculate the $^{13}\text{C}_{\text{ipso}}$ NMR line shape of $4\text{-}^6\text{Li}$ subject to the dynamics of intermolecular carbon–lithium bond exchange.²²

$$\dot{\rho} = i[\rho, \mathcal{H}] - \frac{\rho}{T} + R\rho + E\rho \quad (18)$$

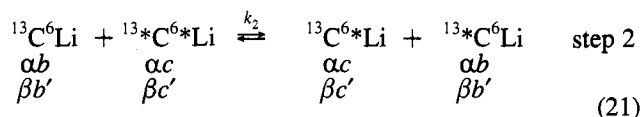
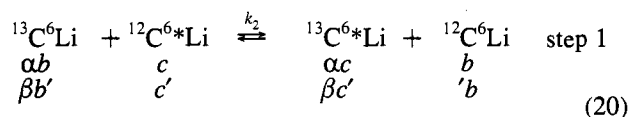
These equations are identical to (8) except the relaxation terms r_d are replaced with elements of the exchange operator $[E\rho]_{ij}$ given as (19).

$$[E\rho]_{ij} = \sum_m \frac{1}{\tau_m} (\rho(\text{aem}) - \rho)_{ij} \quad (19)$$

where m sums over different mechanistic steps, ae means after exchange, and τ 's are mean lifetimes between successive exchanges. The exchanging system $4\text{-}^6\text{Li}$ is enriched >96% in ^6Li and of natural abundance in ^{13}C . As far as NMR of $^{13}\text{C}_{\text{ipso}}$ is concerned the exchanging species may be described as $^{13}\text{C}^6\text{-Li}$ or $^{12}\text{C}^6\text{-Li}$. The bimolecular steps to be considered are (20), the faster one, and (21), abbreviated 1 and 2. They are shown together with the spin functions of pseudospecies "CLi" in the product representation, $\phi_C\phi_{\text{Li}}$. The kinetic isotope effect is neglected.

(22) Reference 14b, Chapters 5 and 6.

(23) Grunwald, E.; Loewenstein, A.; Meiboom, S. *J. Chem. Phys.* **1957**, *27*, 630.



Since we shall solve only for the ^{13}C resonance all matrix elements of $E\rho$ are diagonal in states of ^6Li so that $b = b'$ and $c = c'$. For exchange step 20 an element of ρ^{CLi} is given by

$$\rho_{ab,bb}^{\text{CLi}} = \rho_{ab,bb}^{\text{CLi}} \sum_c \rho_{c,c}^{\text{Li}*} \quad (22)$$

since $\text{Tr}\rho = 1$. Then the after (ae1) exchange elements of step 2 are obtained by permuting b with c in the subscripted states and Li and Li* in the chemical label.

$$\begin{aligned} (\rho(\text{ae1}))_{ab,bb} &= \sum_c \rho_{ac,bc}^{\text{CLi}*} \rho_{b,b'}^{\text{Li}} \\ &= \frac{1}{3} \sum_c \rho_{ac,bc}^{\text{CLi}} \end{aligned} \quad (23)$$

Since ^6Li has three spin states a diagonal element of ρ^{Li} is $1/3$. Note that the asterisk can be removed from the chemical label. In similar fashion for the slower exchange step, (21), the before exchange term is given as (24).

$$\rho_{ab,bb}^{\text{CLi}} = \rho_{ab,bb}^{\text{CLi}} \sum_{dc} \rho_{dc,dc}^{\text{CLi}} \quad (24)$$

After exchanging via step (21) (ae2) an element of ρ^{CLi}

$$(\rho(\text{ae2}))_{ab,bb} = \sum_c \rho_{ac,bc}^{\text{CLi}} \sum_d \rho_{db,db}^{\text{CLi}} \quad (25)$$

becomes (25).

There are two states, d , of ^{13}C and six of $^{13}\text{C}^6\text{Li}$, hence the diagonal elements add up to $1/3$ so that (25) simplifies to (26)

$$(\rho(\text{ae2}))_{ab,bb} = \frac{1}{3} \sum_c \rho_{ac,bc}^{\text{CLi}} \quad (26)$$

and an element of $E\rho^{\text{CLi}}$ would be (27), taking account of (20) and (21).

$$(E\rho^{\text{CLi}})_{ab,bb} = \left(\frac{1}{\tau_1} + \frac{1}{\tau_2} \right) \left(\frac{1}{3} \sum_c \rho_{ac,bc}^{\text{CLi}} - \rho_{ab,bb}^{\text{CLi}} \right) \quad (27)$$

Notice the identity of (26) to (23).

Recalling the definition of τ ,²³

$$\frac{1}{\tau_x} = \frac{\text{rate law}}{(X)} \quad (28)$$

The two terms in (27) are given as

$$\frac{1}{\tau_1} = k_2(^{12}\text{C}^6\text{Li}) \quad (29)$$

$$\frac{1}{\tau_2} = k_2(^{13}\text{C}^6\text{Li})$$

The sample of $4\text{-}^6\text{Li}$ contained ^{13}C in natural abundance so that

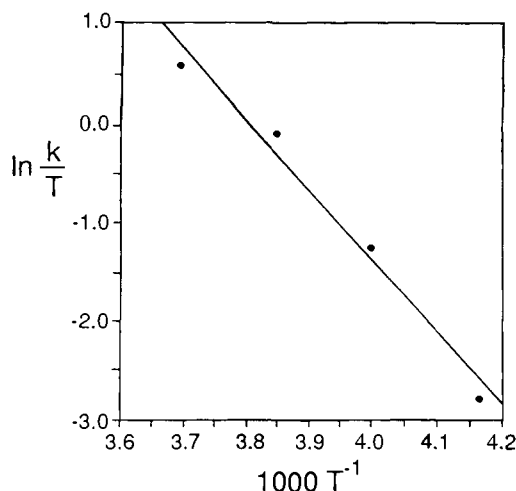


Figure 8. Eyring plot of carbon–lithium bond exchange in 4-⁶Li in THF-D₈.

$1/\tau_1$ is *ca.* $100/\tau_2$, i.e. reaction (20) is 100 times faster than (21). For simplicity the sum of reciprocal τ 's in (27) is replaced by $1/\tau$. Equation 30 exhibits the exchange matrix for ¹³C⁶Li undergoing intermolecular C, Li bond exchange.

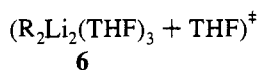
$$\mathbf{E} = \begin{bmatrix} -2/3\tau^{-1} & 1/3\tau^{-1} & 1/3\tau^{-1} \\ 1/3\tau^{-1} & -2/3\tau^{-1} & 1/3\tau^{-1} \\ 1/3\tau^{-1} & 1/3\tau^{-1} & -2/3\tau^{-1} \end{bmatrix} \quad (30)$$

The relaxation part of the coefficient matrix in (8) is replaced by the exchange matrix, (30). The resulting equation is solved for the $\rho_{ab,bb}^{\text{CLi}}$ elements which provide the NMR absorption using (2).

Comparing experimental ¹³C_{ipso} resonances for 4-⁶Li with calculated line shapes (Figure 7) provides the dynamic parameters used in the Eyring plot (Figure 8), which gives ΔH^\ddagger and ΔS^\ddagger values of 14.4 kcal/mol and 7 eu, respectively. Bimolecular exchange



must pass through a dimeric transition state or possibly a dimeric intermediate, see (31). Aggregation among solvated organolithium species is generally accompanied by a decrease in solvation. If development of the transition state, **6**, involves loss of a THF molecule then the molecularity change would be neutral, consistent with a low, in magnitude, ΔS^\ddagger .



Mesityllithium-⁶Li (5-⁶Li) was prepared by halogen–lithium exchange from the bromide using *n*-butyllithium in pentane. Solutions for NMR study were prepared using THF-D₈ alone and THF-D₈ with a molar equivalent of *N,N,N',N',N''*-pentamethyldiethylenetriamine, PMDTA. Carbon-13 shifts for this latter sample at 184 and 298 K are listed in Figure 9. At 184 K the ¹³C_{ipso} resonance is a well-resolved 1:1:1 triplet due to $^1J(^{13}\text{C}, ^6\text{Li})$ of 15 Hz, the signature of a solvated organolithium monomer. At this temperature intermolecular C, Li bond exchange is too slow to average the ¹³C, ⁶Li coupling constant, which confirms the results of the Schleyer group.⁹ The ring carbon shifts at the two temperatures are very similar with some interesting exceptions. The shift ¹³C_{ipso} increases from δ 179.9 at 184 K to δ 191.2 at 298 K. In addition at low temperature the *ortho* methyls and *ortho* ring carbons are all non-equivalent,

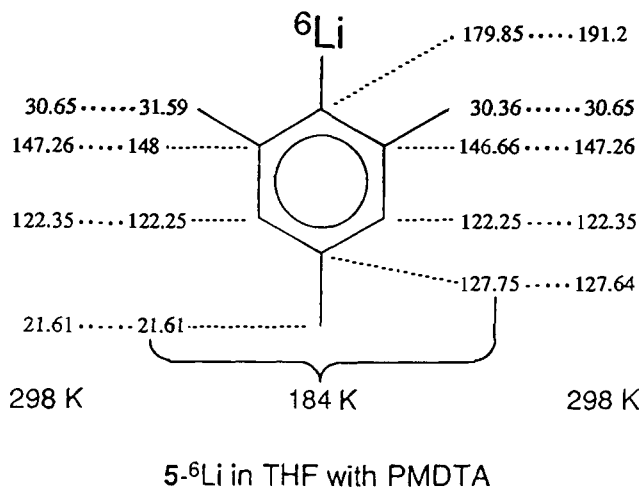


Figure 9. ¹³C NMR mesityllithium-⁶Li · PMDTA shifts, mesityl moiety, at 184 and 298 K.

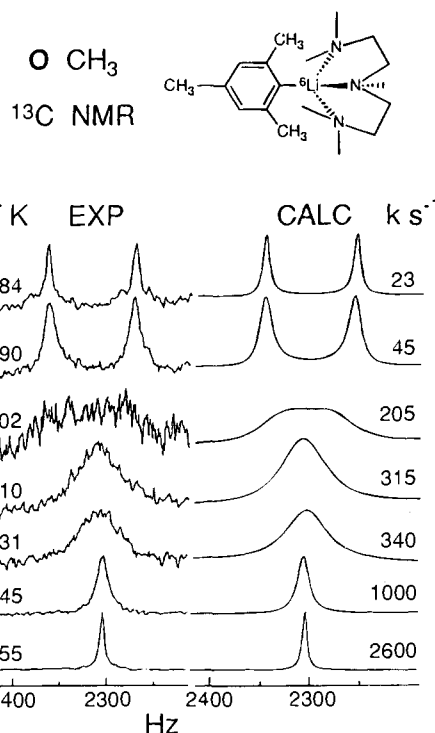


Figure 10. ¹³C NMR line shapes of 5-⁶Li · PMDTA in THF-D₈, *ortho* methyls: (left) experimental at different temperatures; (right) calculated to fit.

giving rise to two well-spaced doublets (see Figures 10 and 11, respectively). This argues for a structure in which the plane of the aromatic ring is unsymmetrically sited with respect to the solvation arrangement about lithium and that rotation about the ring C–Li bond is slow relative to the NMR time scale, i.e., the frequency differences between the *ortho* methyls and *ortho* ring carbons at 184 K. This conclusion is also supported by the appearance of the part of the ¹³C NMR due to PMDTA at 184 K which gives rise to nine peaks of equal intensity, two of which overlap at δ 43 to 44, see Figure 12. *N*-Methyl carbons are distinguished from methylene carbons by the result of a DEPT experiment and by their shifts. Resonances at (δ scale) 57.8, 56.9, 55.2, and 52 are assigned to CH₂ carbons, and those at 48.2, 49.76, 44.2, and 43.13 are due to (dimethylamino)-methyl carbons. Finally the peak at δ 46.4 must be the central *N*-methyl as implied by NMR line shape changes at higher temperatures. The ¹³C shifts of free PMDTA are different from these and are not observed in this spectrum. These results

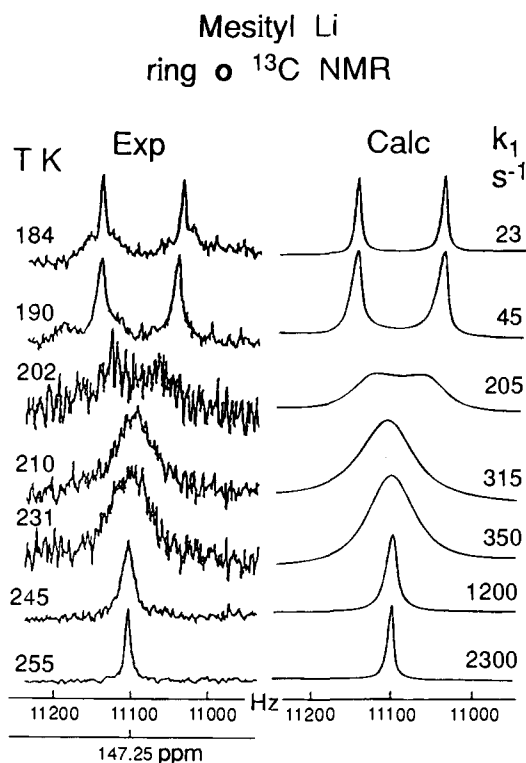


Figure 11. As in Figure 10, *ortho* ring carbon ^{13}C NMR: (left) experimental at different temperatures; (right) calculated to fit.

closely resemble ^{13}C NMR of PMDTA tridentately complexed to neopentylolithium²⁴ and are also consistent with the X-ray crystallographic structure reported by Weiss and co-workers for the phenyllithium PMDTA complex.¹² One can safely conclude that $5\text{-}^6\text{Li}$ in our samples is also tridentately complexed to PMDTA.

Above 184 K there is signal averaging among the PMDTA resonances of $5\text{-Li} \cdot \text{PMDTA}$; δ values, at 57.8 with 56.9 and at 55 with 52 and all the $\text{N}(\text{CH}_3)_2$ resonances coalesce to a broad band at δ 46.1 which also overlaps with the shift for the center NCH_3 (see Figure 12). This pattern of signal averaging of the PMDTA resonances is also very similar to that seen at low temperatures for neopentylolithium complexed to PMDTA.²⁴ By analogy to the results for neopentylolithium the averaging of the four methylene resonances to two in $5\text{-}^6\text{Li} \cdot \text{PMDTA}$ would be the result of rotation of complexed PMDTA around the carbon–lithium bond. Thus signal averaging seen among the (dimethylamino)methyl resonances of $5\text{-}^6\text{Li} \cdot \text{PMDTA}$ would be between peaks (δ units) at 49.3 with 44.2 and 43.9 with 48.2, each pair representing methyl groups on the same side of complexed PMDTA. These assignments are qualitatively consistent with the observed changes in pattern of the ^{13}C dimethylamino resonances. Signal averaging observed in ^{13}C NMR of *ortho* methyls, *ortho* ring carbons, and two pairs of methylenes of PMDTA in $5\text{-}^6\text{Li} \cdot \text{PMDTA}$ also implicates a rotational process around the carbon lithium bond (see Figures 10 and 11). Each of these ^{13}C NMR line shapes, methylene, *ortho* methyls, and *ortho* carbons, was analyzed as a 1:1 two-site uncoupled exchanging system. Figures 10 and 11 show the experimental ^{13}C resonances together with line shapes calculated to fit them for respectively the *ortho* methyls and the *ortho* ring carbons. The resulting rate constants for rotation about the C–Li bond yield activation parameters ΔH^\ddagger and ΔS^\ddagger from the *ortho* ring carbons of 5.1 kcal/mol and -22 eu while

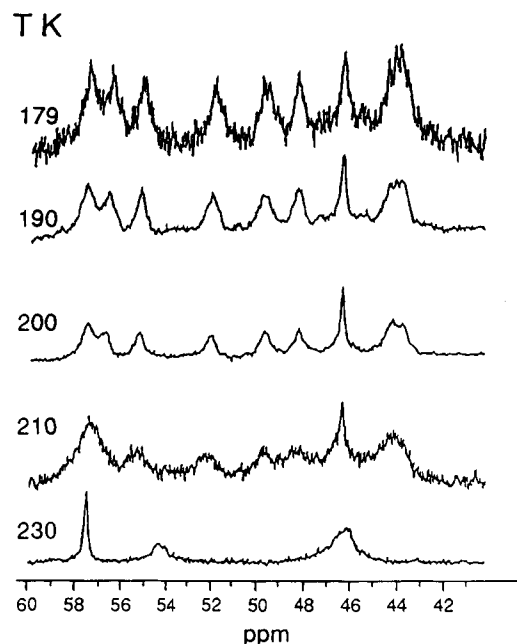
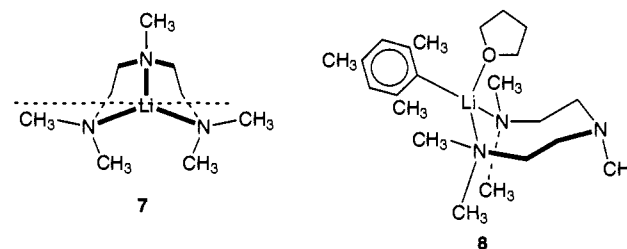


Figure 12. ^{13}C NMR of $5\text{-}^6\text{Li} \cdot \text{PMDTA}$ in THF-D_8 . PMDTA portion, at different temperatures.

from the *ortho* methyl resonance the values are 5.3 kcal/mol and -21 eu, respectively. The methylene resonance of $5\text{-}^6\text{Li} \cdot \text{PMDTA}$ is less well defined than for the aromatic moiety. Line shape analysis yields ΔH^\ddagger and ΔS^\ddagger of 4.7 kcal/mol and -24 eu, respectively. While all these PMDTA line shape changes reflect the rotation process about the C–Li bond, from the quality of the data the most confidence should be placed on the results using the mesityl resonances.

It is now appropriate to inquire into the nature of the process we have loosely called carbon–lithium bond rotation. In principle such a process could be responsible for the averaging of the *ortho* methyls, the *ortho* ring carbon, and the two pairs of methylene, ^{13}C resonances respectively of $5\text{-}^6\text{Li} \cdot \text{PMDTA}$. The simplest transition state is one in which the plane of the aromatic ring parallels the line between the terminal nitrogens of PMDTA, see 7. This would involve strong repulsions between the ring methyls and (dimethylamino)methyls on the same side of the coordinated PMDTA. An alternative process



we would like to propose involves fast reversible dissociation of the central Li–N bond (the most strained one) with concerted uptake of one THF molecule by lithium. Then rotation would take place within the THF complexed intermediate, 8. In such a process N, Li dissociation would increase the entropy. This would be more than counterbalanced by uptake of a molecule of THF. This proposed mechanism avoids the repulsion between methyls and is consistent with the large negative entropy change. Although a dissociative mechanism is likely to be responsible for overall carbon–lithium bond rotation, variations of such a process cannot be excluded. These may include $\text{N}(\text{CH}_3)_2$, Li dissociation, and inversion at nitrogen and at lithium.

(24) Fraenkel, G.; Chow, A.; Winchester, W. R. *J. Am. Chem. Soc.* **1990**, *112*, 6190–6198.

Table 2. NMR Parameters

parameter	carbon-13	lithium-6
spectral freq	75.436	44.148
acquisition size	32K	9K
sweep width, Hz	11363.636	4000
O1	40493.039	1144.531
O2	6000.00	8000.00
acquisition time, s	1.0	8.192
pulse width, μ s	8.5	3
dwelt time, μ s	33	1.25
decoupler power, H	22	22
line broadening, Hz	1.2	1
filter width, Hz	18200	4800

Conclusions

We have shown how ^{13}C NMR of two monomeric aryllithiums, **4** and **5**, reveals hitherto unknown aspects of structure and dynamic behavior. These include the asymmetric nature of the **5**·PMDTA complex, the mechanism of ^7Li relaxation, the dynamics of intermolecular bond exchange, and the mechanism of rotation around carbon–lithium bonds.

Experimental Section

NMR Samples. The 5 mm OD NMR tube attached to a 2 mm straight bore stopcock via a 12/30 standard joint was flamed out under vacuum, filled with argon, and transferred to the glovebox (argon atmosphere). Dry aryllithium compound was weighed in the glovebox and loaded into the NMR tube using a narrow nickel spatula. After the amine ligand was introduced via syringe, the stopcock was reattached and the assembly transferred to the vacuum line. The contents were degassed via three freeze–thaw cycles. Then deuterated solvent (*ca.* 5 mL) was transferred to the tube by bulb-to-bulb distillation. Finally samples were sealed off under vacuum.

NMR. Proton, carbon-13, and lithium-6 NMR spectra were obtained using Bruker AM-200, AM-250, or MSL-300 MHz spectrometers. Carbon-13 spectra were obtained locked on to the deuterated solvent which also served as the reference. Lithium-6 spectra were obtained unlocked due to the proximity of the deuterium to the ^6Li resonance frequencies. Typical instrumental parameters are listed in Table 2.

NMR Line Shape Analysis. Calculations of NMR line shapes as a function of dynamic effects such as relaxation, chemical exchange, and conformational interconversion were carried out following our published procedures.^{14b,22} The maximum uncertainty is 10% for ΔH^\ddagger and 20% for ΔS^\ddagger .

2,4,6-Tri-*tert*-butylbromobenzene.²⁵ The apparatus, a three-necked flask with an addition funnel, a stir bar, and an argon inlet, was charged with a mixture of 1,3,5-tri-*tert*-butylbenzene (2.19 g, 8.9 mmol) and 10 g of phosphorus pentoxide in 20 mL of trimethyl phosphate. Bromine (1.76 g, 0.6 mL, 0.011 mol) in 10 mL of trimethyl phosphate was added and the whole mixture was stirred at 50–60 °C for 24 h. After completion of the reaction, the mixture was poured into water and filtered to yield 2.40 g of 2,4,6-tri-*tert*-butylbromobenzene. Recrystallization from 1:10 chloroform/ethanol yielded 1.6 g of white crystals of 2,4,6-tri-*tert*-butylbromobenzene in 58.3% yield, mp 170–172 °C (lit.²⁵ mp 177–177.5 °C). ^1H NMR (200 MHz, THF- D_8) δ 1.33 (s, 9 H, *p*- $\text{C}(\text{CH}_3)_3$), 1.59 (s, 18 H, *o*- $\text{C}(\text{CH}_3)_3$), 7.45 (s, 2 H, ring

H); ^{13}C NMR (50 MHz, CDCl_3) δ 30.96 (*o*- $\text{C}(\text{CH}_3)_3$), 31.36 (*p*- $\text{C}(\text{CH}_3)_3$), 34.95 (*p*- $\text{C}(\text{CH}_3)_3$), 38.36 (*o*- $\text{C}(\text{CH}_3)_3$), 123.69 (*m*-ring C), 148.42 (*p*-ring C), 148.58 (*o*-ring C).

Phenyllithium- ^6Li .²⁶ The apparatus, a 100 mL schlenk flask equipped with an addition funnel and stir bar, was flame dried under vacuum and taken into the drybox. Distilled bromobenzene (3.01 g, 2.06 mL, 0.019 mol) was introduced into the schlenk flask and *sec*-butyllithium- ^6Li (15.4 mL, 1.3 M, 0.020 mol) in 10 mL of dry pentane was added dropwise over 0.5 h. The mixture was stirred for 24 h. The white solid which was gradually formed was washed with three 10-mL aliquots of dry pentane. The resulting solid was collected by filtration with a sintered glass funnel. After drying, 1.01 g of pure white phenyllithium- ^6Li was obtained as a white solid in 63% yield and was stored in the drybox. ^1H NMR (200 MHz, diethyl ether- D_{10}) δ 6.89 (m, 3 H, *o*- and *m*-H) and 7.87 (d, 2 H, *o*-ring H); ^{13}C NMR (50 MHz, THF- D_8) δ 123.14 (*m*-ring C), 124.97 (*p*-ring C), 144.19 (*o*-ring C), 188.26 (C–Li).

Mesityllithium- ^6Li (5- ^6Li).**²⁶ The apparatus, a 100 mL schlenk flask equipped with an addition funnel and stir bar, was flame dried under vacuum and transferred into the drybox. Distilled 2,4,6-trimethylbromobenzene (1.79 g, 1.37 mL, 8.97 mmol) in 10 mL of dry pentane was introduced into the schlenk flask and *n*-butyllithium- ^6Li (6 mL, 1.30 M, 8.97 mmol) in 10 mL of dry pentane was added dropwise over 0.5 h. The mixture was stirred for 24 h. The white solid which was gradually formed was washed with three 10-mL aliquots of dry pentane. The solid was collected by filtration using a sintered glass funnel. After drying, 1.05 g of pure mesityllithium- ^6Li was obtained as a white solid in 94% yield and was stored in the drybox. ^1H NMR (250 MHz, THF- D_8) δ 2.07 (s, 3 H, *p*- CH_3), 2.32 (s, 6 H, *o*- CH_3), 6.44 (s, 2 H, *m*-PhH); δ ^{13}C NMR (50 MHz, THF- D_8) δ 21.7 (*p*- CH_3), 28.84 (*o*- CH_3), 123.42 (*m*-ring C), 127.55 (*p*-ring C), 149.8 (*o*-ring C), and 179.85 (C–Li).**

2,4,6-Tri-*tert*-butylphenyllithium- ^6Li (4- ^6Li).** Into a 100 mL schlenk tube, previously flame dried under vacuum, equipped with an addition funnel and a stirbar, was introduced, under argon, 2,4,6-tri-*tert*-butylbromobenzene (2 g, 6.15 mmol) in 10 mL of dry oxygen-free diethyl ether. After cooling the system to 0 °C *n*-butyllithium- ^6Li (3 mL, 2.17 M, 6.15 mmol) in pentane was added dropwise over 0.5 h. The mixture was stirred for 2 h at 0 °C. After ether was removed under vacuum, 15 mL of dry pentane was added. The resulting white precipitate was separated by filtration in the drybox using a sintered glass funnel and washed with three 10-mL aliquots of dry pentane. There was formed 1.07 g of 2,4,6-tri-*tert*-butylphenyllithium- ^6Li , in 65% yield. This material was stored in the drybox under argon. ^1H NMR (300 MHz, THF- D_8) δ 1.25 (s, 9 H, *p*- $\text{C}(\text{CH}_3)_3$), 1.32 (s, 18 H, *o*- $\text{C}(\text{CH}_3)_3$), 6.95 (s, 2 H, *m*-H); δ ^{13}C NMR (75 MHz, THF- D_8) δ 34.88 (*p*- $\text{C}(\text{CH}_3)_3$), 39.24 (*o*- $\text{C}(\text{CH}_3)_3$), 116.22 (*m*-ring C), 142.43 (*p*-ring C), 159.29 (*o*-ring C), and 177.09 (C–Li).**

Acknowledgment. This research was generously supported by the National Science Foundation, Grant Nos. CHE 9317298 and CHE 8717746, as was, in part, purchase of the NMR equipment we have used. We thank Dr. Charles Cottrell, Ohio State Chemical Instrumentation Center for his patient expert assistance.

JA950182A

(25) Pearson, D. E.; Frazer, M. G.; Washburn, L. C. *Synthesis* 1976, 621.

(26) Fraenkel, G.; Dayagi, S.; Kobayashi, S. *J. Phys. Chem.* 1968, 72, 953.